

# OPTIMIZATION OF A RICE FIELD CLASSIFICATION MODEL BASED ON THE THRESHOLD INDEX OF MULTI-TEMPORAL LANDSAT IMAGES

Made Parsa <sup>1\*</sup>, Dede Dirgahayu, Sri Harini, Dony Kushardono

Remote Sensing Application Center

Jln. Kalisari No. 8, Pekayon, Pasar Rebo, Jakarta 13710

\*email: made.parsa@lapan.go.id

Received: 5 May 2020; Revised: 12 August 2020; Approved: 14 August 2020

**Abstract.** The development of rice land classification models in 2018 has shown that the phenology-based threshold of rice crops from the multi-temporal Landsat image index can be used to classify rice fields relatively well. The weakness of the models was the limitations of the research area, which was confined to the Subang region, West Java, so it is was deemed necessary to conduct further research in other areas. The objective of this study is to obtain optimal parameters of classification model of rice and land based on multi-temporal Landsat image indexes. The study was conducted in several districts of rice production centers in South Sulawesi and West Java (besides Subang). The threshold method was employed for the Landsat Image Enhanced Vegetation Index (EVI). Classification accuracy was calculated in two stages, the first using detailed scale reference information on rice field base, and the second using field data (from a survey). Based on the results of the analysis conducted on several models, the highest accuracy is generated by the three index parameter models (EVI\_min, EVI\_max, and EVI\_range) and adjustable threshold with 94.8% overall accuracy. Therefore this model was acceptable for used for nationally rice fields mapping.

Keywords: *multi-temporal, EVI, threshold, optimization*

## 1 INTRODUCTION

The Decree of The Ministry of Agrarian Affairs and Spatial Planning (ATR)/Head of National Land Agency (BPN-RI) No.339 of 2018 dated October 8, 2018 shows that the area of rice fields in Indonesia in 2018 was 7,105,145 hectares, down from 7,750,999 hectares in 2013. Meanwhile the 2016 data show that the area of rice fields in South Sulawesi Province was 656,610 Ha of which were irrigated fields and the remaining 40 % (262,767 Ha) were non-irrigated/rainy lowland. The irrigated rice fields consists of 83.5% PI 2 (rice cropping twice a year); 8.0% IP 3 (rice cropping three times a year) and 7.6% PI 1 (rice cropping once a year). The remaining 0.8% are other crops or not

cropped. The distribution of irrigated rice fields is mostly found in Maros, Pinrang, Bone, Sidrap, Luwu, Wajo, East Luwu, and Soppeng Regencies. 64.1% of non irrigated rice fields are PI 1, 32.9% PI 2, 1.3% PI 3, and the remaining 1.6% are other crops or not cropped (South Sulawesi Provincial Government, 2016).

Parsa, *et al.*, 2019 state that rice fields can be easily recognized on optical images because they have different characteristics compared to other land uses. In the original Landsat-8 channel 6 (SWIR),5 (NIR),4 (Red) color composite image, for example, rice fields cropped with rice are easily identified based on key interpretations, with three different types of appearance. Rice fields will appear blue when in a state of

watering/tillage up until the beginning of cropping), will turn green during the vegetative/generative phase and then turn red after harvest/fallow.

Research by Parsa et al. (2013), in cited in Parsa et al. (2019) mentioned that statistical analyzed of the NDVI multi-temporal (mean, maximum, and minimum value) can be used to make RGB image composite. Based on image, demonstrating that they were able to provide a contrasting appearance between rice crops and other crops, due to the real effect of the difference between the maximum and minimum NDVI values. The results of this identification indicate that of the four index values, the mean value is the most significant effect for mapping rice fields compared to the other three indices. Combining the four multi-temporal statistical value (NDVI) criteria can be used for rapid digital mapping of rice fields (rice) with an accuracy of 87.4%.

The research of Chen et al. (2011) used Chinese HJ-1A/B Environmental Satellite Imagery (30 m spatial resolution) to monitor rice cultivation areas in Guangdong province in southern China. Temporal The NDVI characteristics of lowland rice were analyzed in the study to monitor changes in lowland NDVI. Their results indicate that the Chinese Environmental Satellite HJ-1A/B had great potential in developing an operating system to monitor the growth of rice in South China. Research using MODIS and Landsat 8 imagery to map rice in the Panjin Plain, Northeast China produced a map at a spatial resolution of 30m built on pixel-based and phenology algorithms in rice field and wetland areas. A validation test showed high accuracy of rice rice map. Comparison of the map with others showed a high level of consistency and that it provided more detailed information about the

distribution of rice fields because of its higher spatial resolution. The resulting rice map was evaluated with in-situ soil data and Google Earth images. The estimated overall accuracy and coefficient of kappa were 95% and 0.90 respectively (Zhou et al. 2016, in Parsa et al. 2019).

Based on the above description, optimization research and classification parameters of rice fields based on the phenology of rice crops have been developed, as reflected in the vegetation index using EVI (Enhanced Vegetation Index) of multi-temporal Landsat imagery. The purpose of this study is to obtain optimal parameters from the classification model of rice fields based on the phenology of rice crop EVI multi-temporal Landsat imagery. Through the research, it is expected that optimal parameters and thresholds can be obtained for the classification of rice fields in order to support the operational activities of monitoring rice phases more accurately.

## **2 MATERIALS AND METHODS**

### **2.1 Location and Data**

The study was conducted by taking the objects of several districts in the provinces of South Sulawesi and West Java. The data used were every scene during one year (2018) of Landsat-8 data from USGS in the Google Earth Engine (GEE) Cloud System. In addition, supporting data were used, namely detailed scale (1: 5000) maps of rice fields from the national Mapping Agency (BIG, 2017) and data from field survey results.

### **2.2 Standardization of Data**

The satellite data used is the atmospherically corrected surface reflectance of the Landsat 8 OLI/TIRS sensors from USGS which can be accessed using the GEE platform. These

images contain five visible and near-infrared (VNIR) bands and two short-wave infrared (SWIR) bands, processed to orthorectify surface reflectance, and two thermal infrared (TIR) bands processed to orthorectify brightness temperature.

Vegetation Index of EVI can be obtained by using the following formula :

$$EVI = 2.5 \times \frac{\rho_{nir} - \rho_{red}}{\rho_{nir} + 6 \times \rho_{red} - 7.5 \times \rho_{blue} + 1} \quad (2-1)$$

If Red < NIR OR Blue < Red Else  
 $EVI = 1.5 \times (NIR - Red) / (0.5 + Nir + Red)$   
 (Kontgis *et al.*, 2015; Dong *et al.*, 2016; Zhou *et al.*, 2016; Dirgahayu, D., 2016)

### 2.3 Methods

The research is a follow-up study, therefore the method used follows that of the previous research (Parsa *et al.*, 2019). Method development was undertaken by conducting further analysis of pixels that were not included in the rice field class (adjustment). The phased examination of the classification results was based on the range of EVI values of the mean and standard deviations, assuming the distribution was close to normal. The statistical value of each parameter (EVI Max, EVI Min, EVI Range, and EVI Mean) was calculated on the LBS that is definitely known to be a rice field. The range of EVI

parameter values used are presented in Table 2-1. The results of the classification of each combination of parameters were tested in two stages, first using the reference data for Rice Field Base (LBS) and second using survey data (Kushardono, 2017; Hestie *et al.*, 2017). Considering the results of the classification and reference data have a raster format, the test is raster to raster. While the field data is point data, the second stage is a point to point test by paying attention to the 8 pixels around it, forming a 3x3 pixels area of satellite data used. The LBS reference data used in 2017 were the result of verification by a team led by BIG (BIG, 2017). Field data in this study were obtained in two ways: first, a field survey conducted in the South Sulawesi region, which included 358 sample points in ten districts. Field data retrieval was made by direct and indirect observation (using drones). Verification for the West Java region was made by comparing the results of the classification with Google data in four districts. The sample points were made using the Systematic Random Sampling method. The first point was determined randomly while the next point is determined systematically with a distance of 2.5 km south-north and west-east (Figures 2-1 and 2-2).

Table 2-1: Range of EVI parameter values

Parameter	1 Stdev.		1.5 Stdev.		2.0 Stdev.		2.5 Stdev.		Adjustment	
	Lower limit	Upper limit	Lower limit	Upper limit	Lower limit	Upper limit	Lower limit	Upper limit	Lower limit	Upper limit
EVI_Min	-0.113	0.170	-0.184	0.241	-0.254	0.311	-0.325	0.382		0.188
EVI_Max	0.373	0.428	0.359	0.441	0.345	0.455	0.331	0.469	0.350	
EVI_Mean	0.177	0.297	0.147	0.327	0.117	0.357	0.087	0.388	0.236	0.400
EVI_Med	0.184	0.301	0.155	0.331	0.126	0.360	0.096	0.389		
EVI_Range	0.243	0.500	0.179	0.565	0.114	0.629	0.050	0.693		

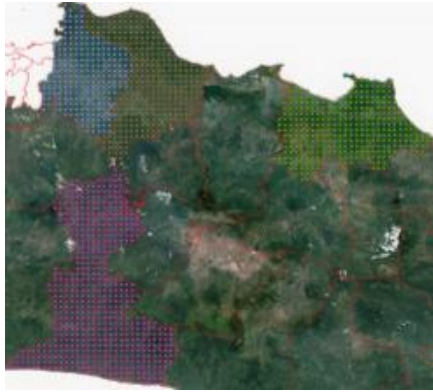


Figure 2-2: Distribution of sample points for West Java (blue, purple, green, and brown points)

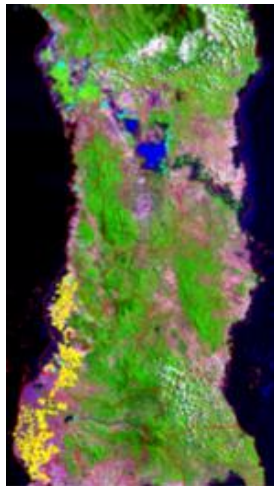


Figure 2-1: Distribution of field sample points for South Sulawesi (yellow and cyan points)

### 3 RESULTS AND DISCUSSION

In the research, several combinations of parameters of EVI statistical value have been conducted and for the classification of rice fields in South Sulawesi and West Java. In the EVI composite image of rice fields planted with rice, these appear green, with bright to dark gradations. This is due to using three EVI values, namely average, maximum and minimum, as shown in Figure 3-1. The results are presented in Figures 3-2 to Figure 3-13.

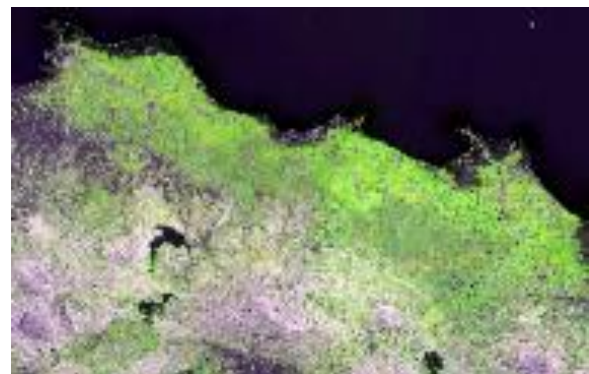


Figure 3-1: West Java multi-temporal composite EVI (mean, max, min) image, January-December 2018

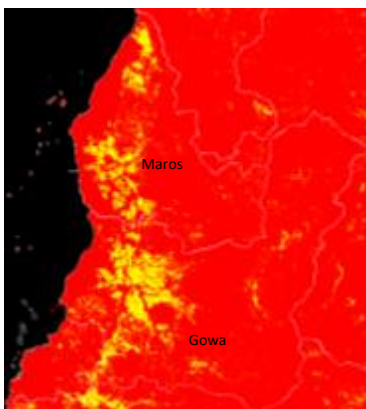


Figure 3-2: Results of the classification of rice fields based on EVI (min, max, mean) stdev 1.0 Maros and Gowa, 2018

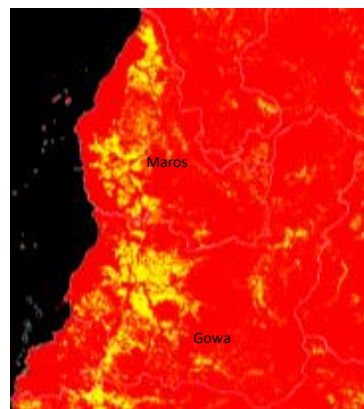


Figure 3-3: Results of the classification of rice fields based on EVI (min, max, mean) stdev 1.5 Maros and Gowa, 2018

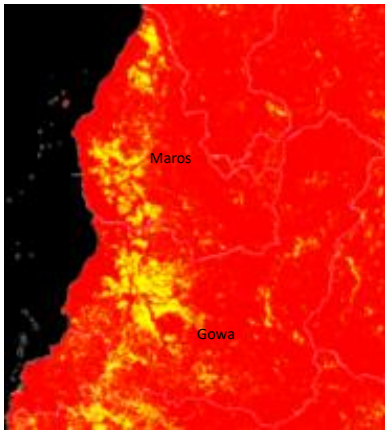


Figure 3-4: Results of the classification of rice fields based on EVI (min, max, range, mean) stdev 1.0, Maros and Gowa, 2018

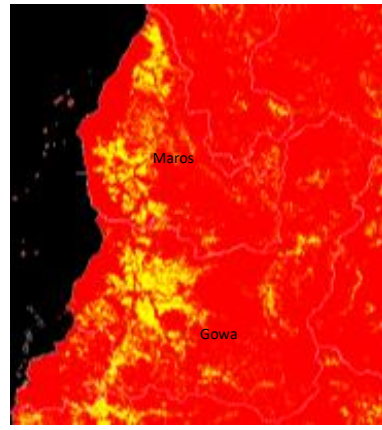


Figure 3-5: Results of the classification of rice fields based on EVI (min, max, range, mean) stdev 1.5, Maros and Gowa, 2018

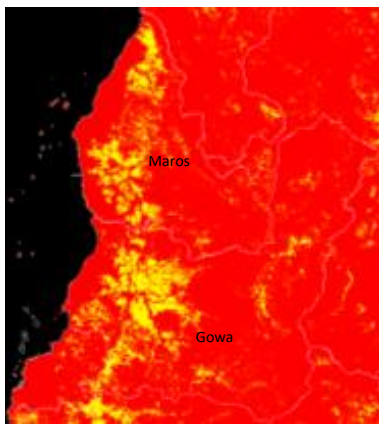


Figure 3-6: Results of the classification of rice fields based on EVI (min, max, mean) threshold are adjusted, Maros and Gowa, 2018

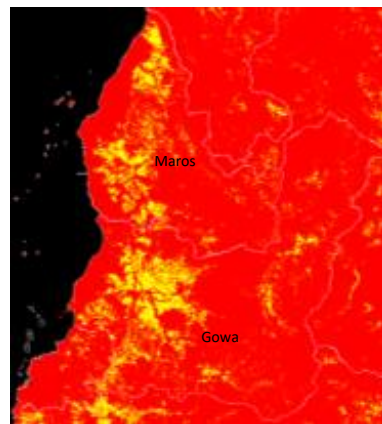


Figure 3-7: Results of the classification of rice fields based on EVI (min, max, range, mean) threshold adjusted, Maros and Gowa, 2018

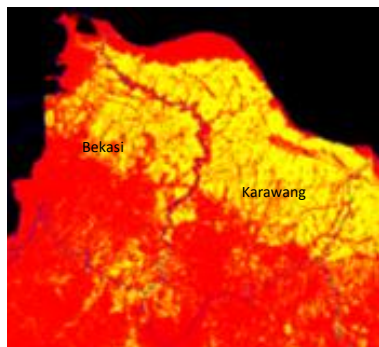


Figure 3-8: Results of the classification of rice fields based on EVI (min, max, mean) stdev 1.0 Bekasi and Karawang, 2018

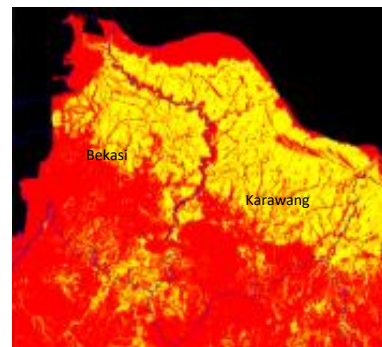


Figure 3-9: Results of the classification of rice fields based on EVI (min, max, mean) stdev 1.5 Bekasi and Karawang, 2018



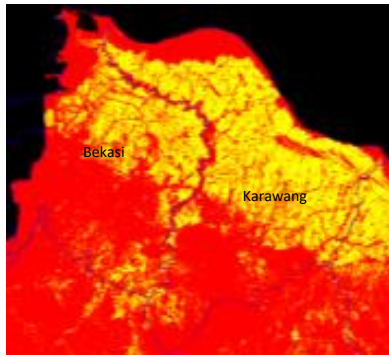


Figure 3-10: Results of the classification of rice fields based on EVI (min, max, range, mean) stdev 1.0 Bekasi and Karawang, 2018

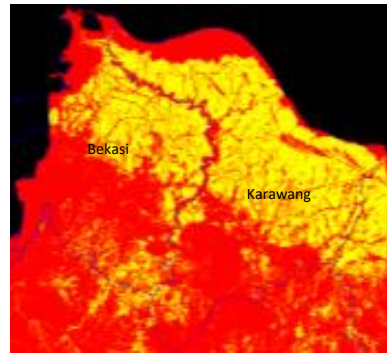


Figure 3-11: Results of the classification of rice fields based on EVI (min, max, range, mean) stdev 1.5 Bekasi and Karawang, 2018

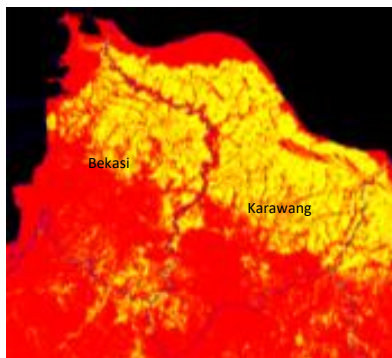


Figure 3-12: Results of the classification of rice fields based on EVI (min, max, mean) threshold adjusted Bekasi and Karawang, 2018

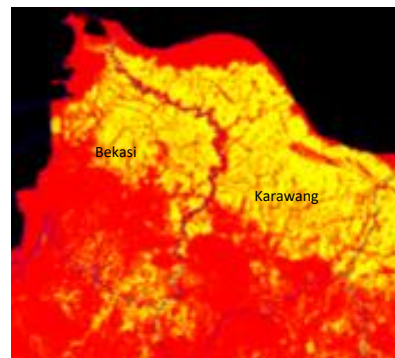


Figure 3-13: Results of the classification of rice fields based on EVI (min, max, range, mean) threshold adjusted Bekasi and Karawang, 2018

**Information:** Area in red: non-rice fields, yellow: rice fields

Examples of the accuracy analysis of the classification results are presented in Tables 3-1 and 3-2.

Table 3-1: Example of accuracy analysis based on LBS

		CLASSIFICATION	
CLASS		Ricefield	Nonrice
LBS	Ricefield	8,917,475*	1,384,475
	Nonrice	130,307	8,949,943
Overall Accuracy		92.18%	

Description \*= pixels

Table 3-2: Example of accuracy analysis based on data sample

		CLASSIFICATION	
CLASS		Ricefield	Nonrice
LBS	Ricefield	455**	26
	Nonrice	1	148
Overall Accuracy		95.71%	

Description \*\*= sum of point sample

The results of the two stages of testing the accuracy of all models are presented in Table 3-3. The table 3-3 above shows that the LBS-based data accuracy has the same tendency, while the three parameter classification model has a higher level of accuracy (although not significant) compared to the four parameter model one. Judging from the standard deviations used, it is seen that 1.5 STDEV results in higher accuracy than the 1.0 threshold. For adjusted threshold treatments, higher accuracy is a result of a combination of three rather than four EVI parameters. This shows that the research has not been able to find the optimal threshold value for the treatment of the four EVI parameters, because logically greater number of

parameters used should produce better accuracy. On the other hand, the classification results tested with the field data show a slightly different trend, with the highest accuracy still from the adjusted threshold treatment (94.75%); followed by the treatment of four EVI parameters (min, max, range, mean) 1.5 stdev at 94.11% then four EVI parameters (min, max, range, mean) threshold adjusted at 93.78%; and with

the lowest treatment being three EVI parameters (min, max, range) 1.0 stdev, at 85.85%.

When viewed as a whole from the results of the two testing techniques, it is shown that in general the classification model tends to be similar to the LBS data. A mismatch between the results of the classification model and LBS can be seen in several locations (Figures 3-13-3-15).

Table 3-3: Accuracy of the rice classification model based on the LBS data and field data for the South Sulawesi and West Java regions

Classification Models	Total Accuracy (%)	
	Based on LBS Data	Based on Field Data
EVI_(min, max, range) 1.0 stdev	91.04	85.85
EVI_(min, max, range) 1.5 stdev	94.73	93.60
EVI_(min, max, range, mean) 1.0 stdev	90.89	86.60
EVI_(min, max, range, mean) 1.5 stdev	90.70	94.11
EVI_(min, max, range), adjustable threshold	94.15	94.75
EVI_(min, max, range, mean), adjustable threshold	93.30	93.78

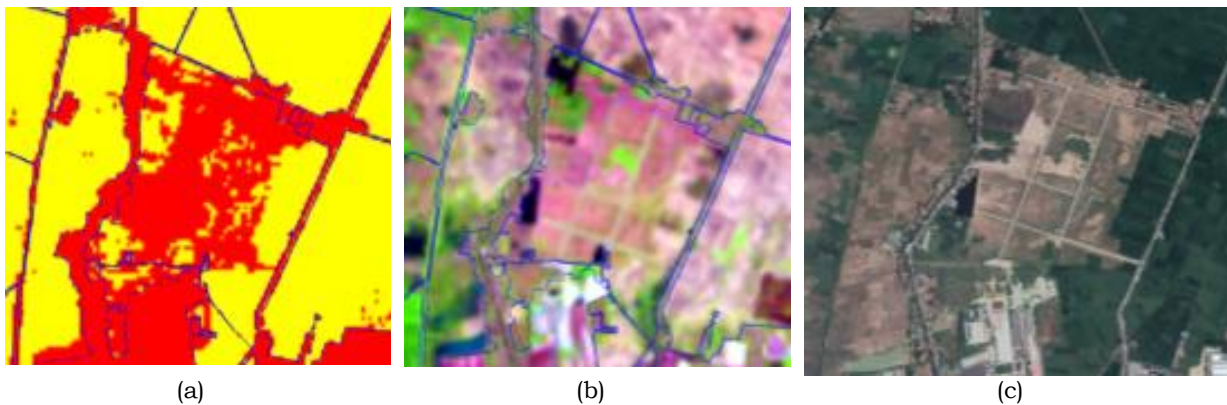


Figure 3-13 (a,b,c): One of the locations where there is a difference between the results of the model classification with LBS; a) the results of the classification are overlapped with LBS (blue vector), b) Landsat-8 imagery September 8, 2018; and c) high resolution imagery (Google, July 7, 2018).



Figure 3-14 (a,b,c): a) high resolution imagery 11 September 2016; b) 12 November 2016; and c) 26 July 2017

Source: Google

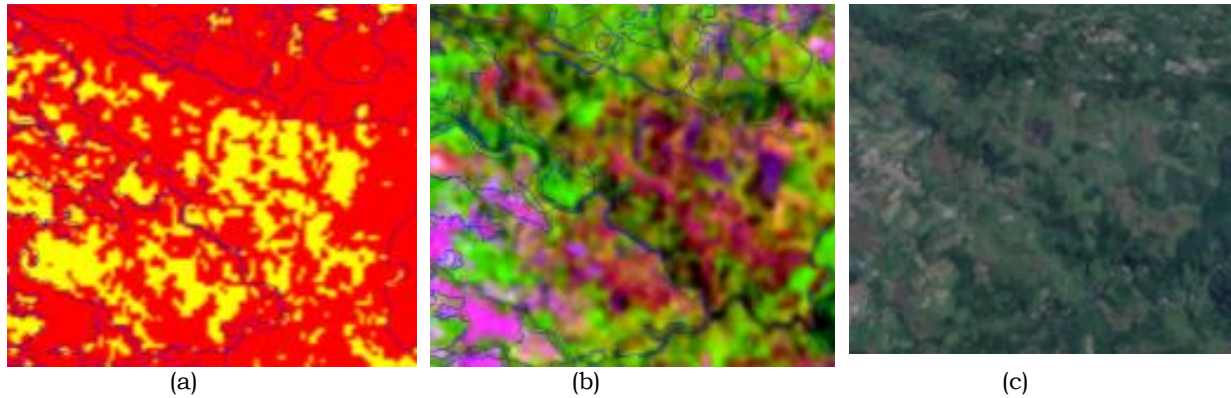


Figure 3-15: One of the two locations where there are differences between the results of the model classification with LBS; a) the results of the classification are overlapped with LBS (blue vector); b) Landsat-8 imagery September 8, 2018; and c) high resolution imagery (Google, July 7, 2018).

The difference here is estimated to be due to its location, being in the process of land conversion, and for which LBS map updates in this section are missing. This is clearly seen from the high resolution data for 2016-2017 (Figure 3-14 a, b, c).

A difference is also seen in the second location (Figure 3-15) which is estimated to be rainfed lowland mixed with non-rice. On the LBS map, this area is used as a class for all rice fields, which can be seen from the high resolution data of 7 July 2018 (Figure 3-15c). It can therefore be concluded that the classification model of rice land based on the multi-temporal Landsat image index is relatively accurate. Maximum accuracy is produced by a three-parameter model (min, max, range) with the following criteria:  $EVI_{Min} \leq 0.344$ ;  $EVI_{Max} > 0.328$ ;  $EVI_{Range} > 0.104$ ; threshold adjusted to an overall accuracy of 94.75%.

#### 4 CONCLUSION

Based on the results of the analysis and discussion that have been presented, it can be concluded that:

a. Optimal parameters were obtained from the classification model of rice fields based on the phenology of rice

crops (EVI vegetation index) multi-temporal Landsat imagery.

b. The optimal parameter for the classification of rice fields is use of the EVI min, max, range with adjusted threshold.

c. More in depth study needs to be conducted to obtain the optimal combination of parameters and thresholds to produce maximum classification accuracy.

#### ACKNOWLEDGMENTS

The author grateful for the collaboration of all the parties who helped conduct the research, including the Remote Sensing Data and Technology Center, which provided satellite imagery data; the Program Fields and Remote Sensing Utilization Centers, which helped with survey equipment; and its operators and resource people from BPTP South Sulawesi, who helped with the field data collection.

#### AUTHOR CONTRIBUTIONS

Optimization Of A Rice Field Classification Model Based On The Threshold Index Of Multi-Temporal Landsat Images. Lead Author: I Made Parsa and Dede Dirgahayu. Co-Author: Sri Harini and Dony Kushardono.



**REFERENCES**

- Badan Informasi Geospasial, (2017), *Kick off meeting rice fields verification*. Available at: <http://www.big.go.id/berita-surta/show/>. Accessed 25 January 2018
- Dirgahayu, D., Noviar, H. dan Anwar, S., (2014), *Model pertumbuhan tanaman padi di pulau sumatera menggunakan data EVI modis multi-temporal*. Seminar Nasional Penginderaan Jauh Tahun. 21 April 2014. IPB International Convention Center. Bogor.
- Dirgahayu, D., (2016). The new method for detecting early cropping and bare land condition in rice field by using vegetation-bare-water index. Proceedings of the 2<sup>nd</sup> International conference of Indonesian Society for Remote Sensing (ICOIRS), 2016, Yogyakarta. ISBN: 978-602-73620-1-7, 331-142.
- Dong, J., Xiao, X., Menarguez, M.A., Zhang, G., Qin, Y., Thau, D. ... More, B. III, (2016). Mapping rice rice cropping area in northeastern asia with landsat 8 images, fenologi-based algorithm and Google Earth Engine. *Remote Sensing of Environment* 185 (2016), 142-154.
- Hestie, T., Tibshirani, R., & Fridman, J., (2017). *The elements of statistical learning data mining, inference, and prediction*. (2<sup>nd</sup> Ed.). Stanford, California: Springer.
- Kontgis, C., Schneider, A., Ozdogan, M. (2015). Mapping rice rice extent and intensification in the Vietnamese mekong river delta with dence time stacks of Landsat data. *Remote Sensing of Environment* 169 (2015), 255-269.
- Kushardono, D. (2017). *Klasifikasi Digital Pada Penginderaan Jauh*. Cetakan 1, November 2017. IPB Pres. Bogor. 75 p.
- Parsa, I.M. & Dirgahayu, D., (2013). Multi-temporal vegetation index of Landsat image analysis for rice field quick mapping (rice crop), case study of Tanggamus, Lampung. *Internasional Journal of Remote Sensing and Earth Sciences*. 10(1), 19-24.
- Parsa, I.M. & Dirgahayu, D. dan Harini, S. (2019). *Pengembangan metode klasifikasi lahan sawah berbasis indeks citra landsat multiwaktu*. *Jurnal Penginderaan Jauh Dan Pengolahan Data Citra Digital*, 16(1), 35-44.
- Pusat Teknologi dan Data Penginderaan Jauh, Lembaga Penerbangan dan Antariksa Nasional. Available at: [www://bdpjn-catalog.lapan.go.id/catalog/index.php](http://www.bdpjn-catalog.lapan.go.id/catalog/index.php), Accessed 31 January 2019.
- Qin, Y., Xiao, X., Dong, J., Zhou, Y., Zhu, Z., Zhang, G. ... Li, X. (2015). Mapping rice rice cropping area in cold temperate climate region through analysis of time series Landsat 8 (OLI), Landsat 7 (ETM+) and MODIS imagery. *ISPRS Journal of Photogrammetry and Remote Sensing* 105 (2015), 220-233.
- South Sulawesi Provincial Government, (2016). *Luas lahan sawah menurut Kabupaten/Kota (hektar)*. Available at: <https://sulselprov.go.id/upload/files/1-Lahan%20Sawah%20Total.pdf>. Accessed 14 November 2019.
- Zhou, Y., Xiao, X., Qin, Y., Dong, J., Zhang, G., Kou, W. ... Li, X. (2016). Mapping rice rice cropping area in rice-wetland coexistent areas through analysis of Landsat 8 OLI and MODIS images. *International Journal of Applied Earth Observation and Geoinformation* 46, 1-12.

